

Supplemental Materials

Notch inhibition overcomes resistance to tyrosine kinase inhibitors in EGFR-driven lung adenocarcinoma

Emilie Bousquet-Mur, Sara Bernardo, Laura Papon, Maicol Mancini, Eric Fabbrizio, Marion Goussard, Irene Ferrer, Anais Giry, Xavier Quantin, Jean-Louis Pujol, Olivier Calvayrac, Herwig P. Moll, Yaël Glasson, Nelly Pirot, Andrei Turtoi, Marta Cañamero, Kwok-Kin Wong, Yosef Yarden, Emilio Casanova, Jean-Charles Soria, Jacques Colinge, Christian W. Siebel, Julien Mazieres, Gilles Favre, Luis Paz-Ares, Antonio Maraver

Supplemental Table 1

Supplemental Figure 1

Supplemental Figure 2

Supplemental Figure 3

Supplemental Figure 4

Supplemental Figure 5

Supplemental Figure 6

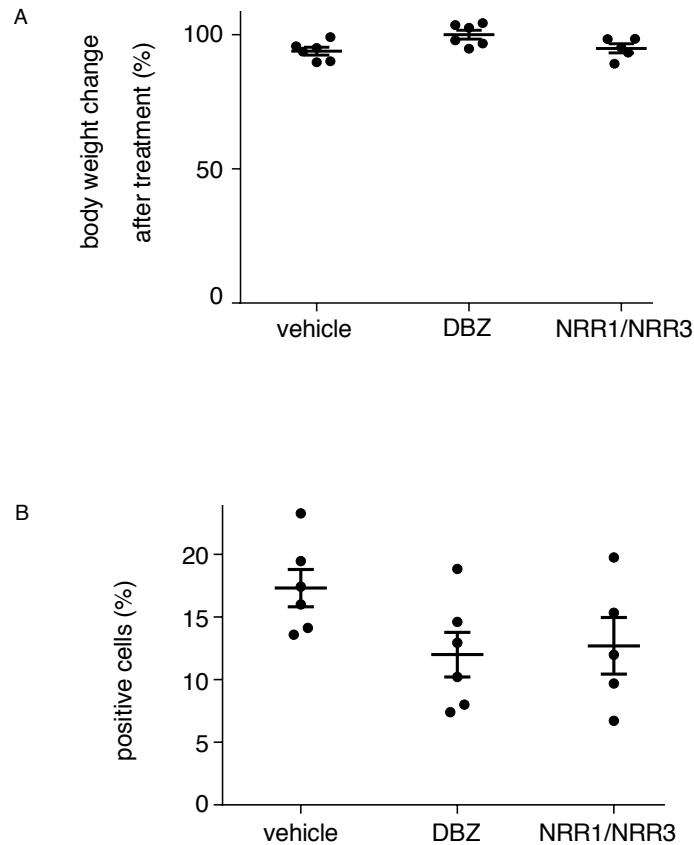
Supplemental Figure 7

Supplemental Figure 8

| pathway | pval | padj | ES | NES | nMoreExtrer | size |
|--|----------------------|----------------------|--------------------|-------------------|-------------|------|
| HALLMARK_MYC_TARGETS_V2 | 3.66568914956012e-05 | 0.000366568914956012 | -0.571841185842812 | -2.03052920663009 | 1 | 58 |
| HALLMARK_TNFA_SIGNALING_VIA_NFKB | 1.76211453744493e-05 | 0.000222190621778236 | -0.454736566115785 | -1.94272679216512 | 0 | 191 |
| HALLMARK_INFLAMMATORY_RESPONSE | 1.77374153038419e-05 | 0.000222190621778236 | -0.433177734599041 | -1.81281063881849 | 0 | 163 |
| HALLMARK_EPITHELIAL_MESENCHYMAL_TRANSITION | 1.77386738567425e-05 | 0.000222190621778236 | -0.423535999716905 | -1.77713182793385 | 0 | 166 |
| HALLMARK_KRAS_SIGNALING_UP | 1.77752497422589e-05 | 0.000222190621778236 | -0.425862435413622 | -1.7737890280657 | 0 | 157 |
| HALLMARK_UV_RESPONSE_DN | 0.000304092730394963 | 0.00253410608662469 | -0.407250154110172 | -1.66584002362953 | 16 | 137 |
| HALLMARK_INTERFERON_ALPHA_RESPONSE | 0.00341296928327645 | 0.0170648464163823 | -0.41529577496119 | -1.59216161787522 | 187 | 90 |
| HALLMARK_GLYCOLYSIS | 0.000951592154651347 | 0.00594745096657092 | -0.362629891577758 | -1.54595052700103 | 53 | 188 |
| HALLMARK_KRAS_SIGNALING_DN | 0.00258403789922252 | 0.0143557661067918 | 0.373475170892941 | 1.55131646149907 | 113 | 132 |

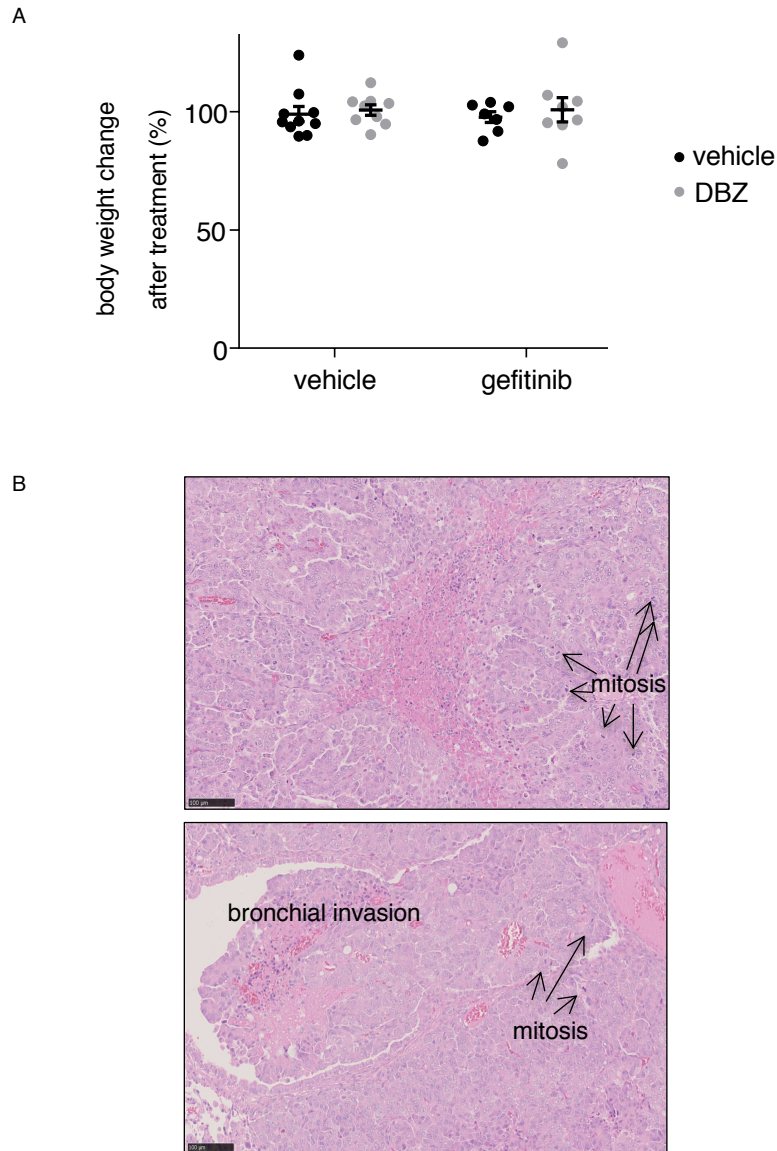
Supplemental Table 1. Gene sets altered in PC9GR cells upon incubation with gefitinib.

PC9GR cells were serum-starved for 18h and then treated with vehicle (DMSO) or gefitinib (1 μ M) for 6h. RNA was extracted and analyzed by RNA-seq (n = 3 per condition; FDR < 0.001).



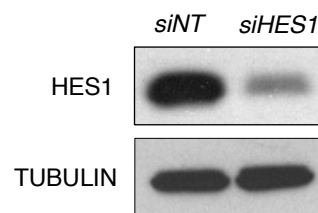
Supplemental Figure 1. Treatment schedules do not affect the weight of animals, and AKT phosphorylation status is not altered by Notch inhibition.

(A). Treatment with DBZ and the NRR1/NRR3 antibodies does not affect the weight of mice compared with controls. Animals treated with vehicle (methocel and IgG, n = 6), DBZ (GSI, n = 6), or NRR1/NRR3 (anti-NOTCH1 and anti-NOTCH3 antibodies, n = 5) were weighted the first and last day of treatment and the change in body weight is shown. (B) Immunohistochemical analysis of pAKT in lung tumors from mice treated with vehicle (methocel and IgG, n = 6), DBZ (GSI, n = 6), or NRR1/NRR3 (anti-NOTCH1 and anti-NOTCH3 antibodies, n = 5). In A and B values correspond to the mean \pm S.E.M. Statistical significance was determined by one-way ANOVA test followed by Tukey's post hoc test, but results were not significantly different.



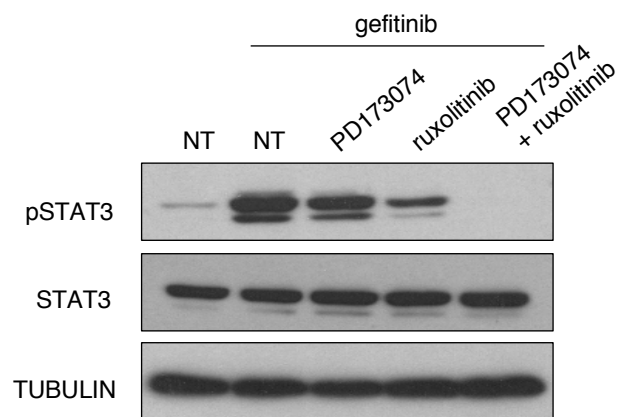
Supplemental Figure 2. Treatment schedules of DBZ and/or gefitinib do not alter the weight of animals, and examples of lung adenocarcinomas in *EGFR*^{T790M/L858R} mice.

(A) Effect of the DBZ and gefitinib treatments on the weight of mice. Mice treated with vehicle (methocel, n = 9), DBZ (n = 10), gefitinib (n = 7), and DBZ+gefitinib (n = 8) for 5 weeks were weighted the first and last day of treatment, and the change in body weight is shown. Statistical significance was determined by one-way ANOVA test followed by Tukey's post hoc test, but results were not significantly different. (B) Representative images of lung adenocarcinoma in *EGFR*^{T790M/L858R} mice. After H&E staining, lung adenocarcinomas were identified and quantified. Here are two examples of lung adenocarcinomas with classic citoarchitectural histological features, such as invasion and high mitotic rate. Black arrows indicate some mitosis.



Supplemental Figure 3. *siHES1* treatment reduces HES1 levels.

PC9GR cells were transfected with 20 nM of non-targeting siRNA (*siNT*) or a siRNA targeting *HES1* (*siHES1*). 48h after transfection, proteins were extracted and analyzed by western blotting with antibodies against the indicated proteins. This is a representative image of three different experiments.



Supplemental Figure 4. Gefitinib induces STAT3 activation through FGFR and JAK.

PC9GR cells were treated with PD173074 (2 μM) or/and ruxolitinib (0.25 μM) for 24h. Gefitinib was added (1 μM) for the last 6h. Then, proteins were extracted and analyzed by western blotting with antibodies against the indicated proteins. This is a representative image of two different experiments.

A

HUMAN HES1 PROMOTER

acgccggccgctgatgtcaaaactgcagctcggctggtgtagctcttaaa
 gggcccgcggcgccggggccgaggcccgcccgggcgaggaggaga
 ggctgcttccctgcccgccacctcaacgcgcccgcagaacctaaagcctac
 ggatgaaaaggaaaggggtggaaggagggcgcgagctccctgagtcatt
 gccctcggagcccccttgttcattttttcatttgaaataccgtttcctt
 ccacccagttggaaattattctgattgtttcctggggaagcccggggtct
 aaggccccaaatccaaacgaggaatttctgaaagacgggtgggggtggg
 attcaagaactaccttgctccgaaaaacctgcatttgtgaggtagaaggc
 aatttttcctttttctgcatggaaacaggaatttttttgccccttttc
 ctttaccatctactttcaccctcctgaatgtaaagtctgagcgggaactt
 tagatgtgtcggtaactcacattcttacacccgtccccctccccgc
 ccccttttaaccactgctgttttttctttattgtttataacctt**taaaaa**
aaatattgtttcaaatgaacttactacagtcaaagcagctctgttacatat
 gagagaggcataaagagcaaagaccctggctccaaaagaaatagacaag
 atcaagaccaaagcggaaagaaaaaaaaaatctctaaaccaagcccaga
 gggagagttagcaaaggggttaaaatccttttgattgacgtgtgagcctccg
 gtgccctgggctcaggcgcgccattggcccgccagacctgtgectggc
 ggccaatggggggcgcggtccacgagcgggtgcccgtgtctcctctcc
 ca**ttggctgaa**agtt**actgtgggaaag**aaagtttgggaa**gtttcacacga**
gccgttcgctgcagctccagatatatatagaggccgcccaggccctaggg
 ATCACACAGGATCCGGAGCTGGTCTGATAACAGCGGAATCCCCCGTCTA
 CCTCTCCTTGGTCTGGAACAGCGCTACTGATCACCAAGTAGCCACAA
 AATATAATAAACCTCAGCACTTGCTCAGTAGTTTTGTGAAAGTCTCAAG
 TAAAAGAGACACAAAACAAAAAATCTTTTTCGTGAAGAACTCCAAAAATA
 AAATTCTCTAGAGATAAAAAAAAAAAAAAAAAAGGAAATGCCAGCTGATAT

RBPJ
STAT3
 ATG CDS

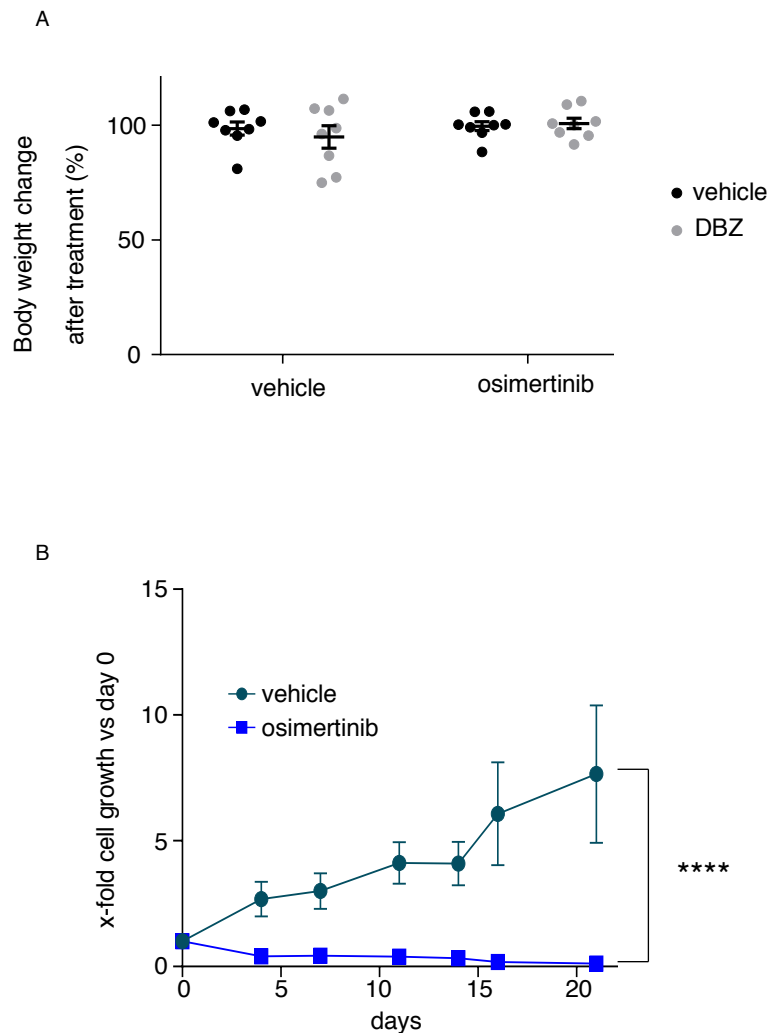
B

MURINE HES1 PROMOTER

caggcgcgcctcgcggcggctgatgtcaaaactgcagctcggctggtg
 gagctcttaaagggctcgcgcgcccggcgccgaggccgcttgccgcgcc
 gcggggtagaggaggagagcccgactcccttgcccgcgctctatccgt
 attgccaaactgggagcctgcccggagaaaggttagagagagtgccggaggga
 acgagcgcgcccctcctgtgcattgtctatcaaagcccccttgttcatt
 tttttttcgtttgaaattccatttctttctgcccagtaggaaattatt
 ctgattgtttctggagaagcgtgaggtccaaggttgcaattccaagaga
 ggaatgaaatgggctagaggagacaagcatccaaaagacaccttgctccg
 aaaacctggctgtgaaggcatttggggggacggttaagggcatgtttagc
 gtgtgggggttagtatctcccaacctcatgagcagttttgactccccta
 aacatacagagttcagagcgggaattccggaagaca**tttagagtaa**cacatc
 ctctttaccttgttccctcc**tttttcaa**tcactaaattttgtcttgcc
 tatactgttcaaaaata**tttttcaa**tgaactta**ttatacaaa**gtagtta
 tattgcatgcagcaagaacaataaaaaccaaaggcctggccacaaaagaa
 atagactagactaaaactaagcaaaagccagaggaaaggttagcaaaagg
 gttaaaatccttttgattgacgtgtgagcctccgggtgcccgggctcagg
 cgcgcgccattggccgcccagacctgtgacctagcggccaatggggggcg
 cagtcacagcgggtgcccgtgtctcttccctcca**ttggctgaa**agtt**a**
ctgtgggaaagaaagtttgggaa**gtttcacacga**ccgttcgctgcagc
 ccagatatatatagaggccgcccaggccctgcccgatcacacaggatctgg
 AGCTGGTCTGATAACAGCGGAATCCCCTGTCTACCTCTCTCCTTGGTCC
 TGGAATAGTGTACCGATCACTAAGTAGCCCTAAGACATAATAAACCTTC
 AACTGCTCAGTAGTTTTTCTTATGAAAAGTCAAGTAAAAGGACGTAAGCAA
 AAAAAAATATTTTTTTTTTTCGTGAAGGATTCCAAAAATAAAATCTCT
 GGGGACTGAGAAGAAAAAAAAAAAAAAAAACGAAATGCCAGCTGATATAA

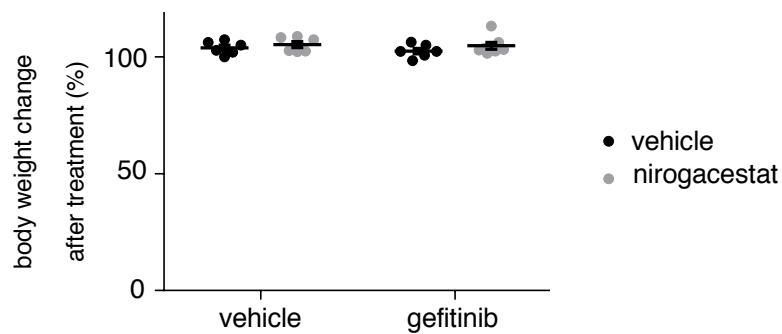
Supplemental Figure 5. Human *HES1* and murine *Hes1* promoter sequences.

(A) Murine *Hes1* and (B) human *HES1* promoter sequences. The consensus binding sites for RBPJ and STAT3 are highlighted in red and light blue, respectively. Dark blue letters indicate where the coding sequences (CDS) of both genes start.



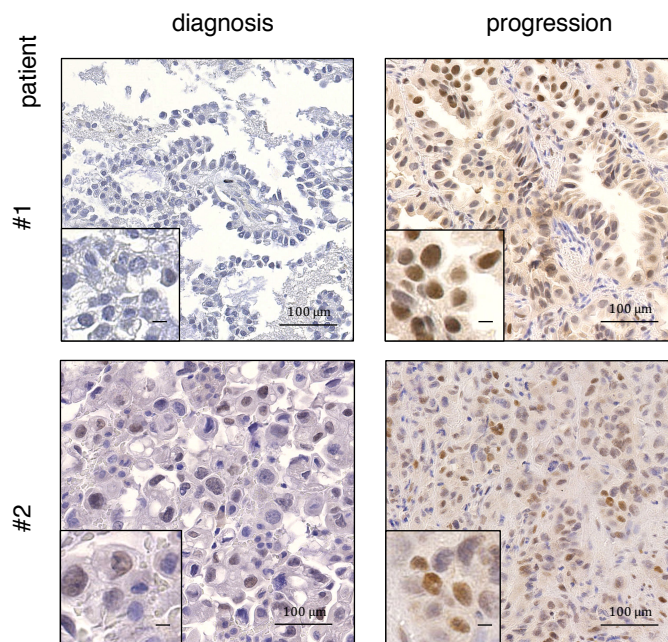
Supplemental Figure 6. Treatment schedules of DBZ and/or osimertinib do not alter the weight of animals.

(A) Mice treated with vehicle (methocel, $n = 8$), DBZ ($n = 8$), osimertinib ($n = 8$), or DBZ/osimertinib ($n = 7$) for 5 weeks were weighted the first and last day of treatment, and the change in body weight is shown. Values correspond to the mean \pm S.E.M. Statistical significance was determined by one-way ANOVA test followed by Tukey's post hoc test, but results were not significantly different. (B) 3.5×10^6 PC9GR cells were injected subcutaneously in the right flank of nude mice. Mice were treated with vehicle (methocel, $n = 8$), or osimertinib ($n = 8$). The tumor size was measured twice per week. The y-axis shows the tumor growth fold increase versus day 0 in each treatment and time point. Values correspond to the mean \pm SEM. Statistical significance was determined by a two-way ANOVA test followed by Tukey's post hoc test: **** $p \leq 0.0001$.



Supplemental Figure 7. Treatment schedules of nirogacestat and/or gefitinib do not impact on the weight of animals.

Mice treated with vehicle (methocel, n = 6), nirogacestat (n = 6), gefitinib (n = 6), or nirogacestat+gefitinib (n = 7) were weighed the first and last day of treatment, and the change in body weight is shown. Values correspond to the mean \pm S.E.M. Statistical significance was determined by one-way ANOVA test followed by Tukey's post hoc test, but results were not significantly different.



Supplemental Figure 8. Examples of immunohistochemical analysis of HES1 expression in patient biopsies of lung adenocarcinoma.

HES1 staining in lung adenocarcinoma tissue sections from two patients with an EGFR-mutated cancer before TKI treatment (diagnosis) and after relapse. Scale bar at insets = 25µm.